

field dwarfs, strengthens the case for the youth of Oph 1622-2405AB.

There is no consensus yet on the origin of free-floating substellar objects. One possibility is that they form like higher mass stars, as a result of the turbulent fragmentation and collapse of molecular cloud cores (20). Another scenario, which has gained popularity in recent years, is that brown dwarfs are stellar embryos ejected from multiple protostellar systems (9, 10). Recent observations have attempted to distinguish between these scenarios by comparing the physical properties of substellar objects with those of Sun-like stars. A variety of studies have shown that many young brown dwarfs and planetesimals exhibit infrared excesses (4, 6, 7, 11) and spectroscopic signatures of accretion (5, 8), indicative of disks. However, these diagnostics are only sensitive to the innermost portions of the disk and therefore cannot test whether brown dwarf disks are truncated, as expected in the ejection scenario, as a result of close dynamical encounters. Recently, Scholz *et al.* (21) found evidence for >10-AU disks among ~25% of Taurus brown dwarfs, contrary to predictions of certain ejection simulations (10), but the test is still somewhat indirect.

In this context, the binary properties of substellar objects could be among the most important diagnostics of their origin. In particular, ejection models predict a very low rate of binaries among brown dwarfs (<5%) and do not favor the formation of wide (>20-AU) binaries (9, 10). Imaging surveys of (old) brown dwarfs in the solar neighborhood reveal that ~15% are in binaries with maximum separations of ~20 AU (22, 23). The same appears to hold true for brown dwarfs in star-forming regions and young open clusters (24, 25), with a few notable exceptions (26–28). The dearth of wide binaries is consistent with ejection models, but the overall binary fraction is higher than predicted by some hydrodynamical simulations of that scenario (10).

Therefore, our identification of an ultra-low-mass binary with a projected separation of ~242 AU is surprising. The high mass ratio of Oph 1622-2405AB is consistent with the bias toward approximately equal mass pairs seen in the substellar regime, but its wide separation is contrary to the general trend toward tighter binaries at the lowest masses. We propose that Oph 1622-2405AB is unlikely to have survived ejection from a multiple protostellar system because such a dynamical interaction would have torn apart a softly bound pair (9, 10). Given its fragility, a future close encounter with a passing star or a brown dwarf could still disrupt this binary.

The lowest mass binary known previously is 2MASSW J1207334-393254, a young ~25  $M_{\text{Jupiter}}$  brown dwarf with an ~8  $M_{\text{Jupiter}}$  companion at a separation of ~55 AU (28). Given its high mass ratio and wide separation, several authors have argued that this pair most likely formed as a petite version of stellar binaries

through cloud fragmentation, instead of the planetary companion forming by means of core accretion in a disk around the primary (29). The same arguments apply even more strongly to Oph 1622-2405AB, given that its mass ratio is higher and its separation is wider. This binary is analogous in some ways to 2MASS J11011926-7732383AB in Chamaeleon I with a mass ratio of 0.5 and a separation of 240 AU, although its components have higher masses of ~50 and ~25  $M_{\text{Jupiter}}$  (26). Thus, a successful theory of star formation must account for wide binaries composed of brown dwarfs and even planetesimals. On the observational front, the key questions are whether such systems are common or rare and whether binary properties depend on the age or the environment. For example, wide binaries may be more frequent among young brown dwarfs, but more systematic surveys are needed to test this possibility.

#### References and Notes

1. G. Basri, *Annu. Rev. Astron. Astrophys.* **38**, 485 (2000).
2. M. R. Zapatero Osorio *et al.*, *Science* **290**, 103 (2000).
3. P. W. Lucas, P. F. Roche, *Mon. Not. R. Astron. Soc.* **314**, 858 (2000).
4. L. Testi *et al.*, *Astrophys. J.* **571**, L155 (2002).
5. R. Jayawardhana, V. D. Ivanov, *Astrophys. J.*, in press; preprint available online (<http://arxiv.org/abs/astro-ph/0607152>).
6. A. Natta *et al.*, *Astron. Astrophys.* **393**, 597 (2002).
7. R. Jayawardhana, D. R. Ardila, B. Stelzer, K. E. Haisch Jr., *Astron. J.* **126**, 1515 (2003).
8. R. Jayawardhana, S. Mohanty, G. Basri, *Astrophys. J.* **592**, 282 (2003).
9. B. Reipurth, C. J. Clarke, *Astron. J.* **122**, 432 (2001).
10. M. R. Bate, I. A. Bonnell, V. Bromm, *Mon. Not. R. Astron. Soc.* **332**, L65 (2002).
11. K. N. Allers, J. E. Kessler-Silacci, L. A. Cieza, D. T. Jaffe, *Astrophys. J.* **644**, 364 (2006).
12. It was pointed out to us after the *Science Express* publication that the companion was reported independently in K. N. Allers' Ph.D. thesis (30), but we note that it

was not mentioned in the Allers *et al.* paper published subsequently in *Astrophysical Journal* (11).

13. Materials and methods are available as supporting material on Science Online.
14. The comparison spectra for field M and L dwarfs are from <http://dwarffarchives.org>, maintained by J. D. Kirkpatrick.
15. E. L. Martin *et al.*, *Astron. J.* **118**, 2466 (1999).
16. S. K. Leggett *et al.*, *Astrophys. J.* **564**, 452 (2002).
17. G. Chabrier, I. Baraffe, F. Allard, P. Hauschildt, *Astrophys. J.* **542**, 464 (2000).
18. I. Baraffe, G. Chabrier, F. Allard, P. Hauschildt, *Astron. Astrophys.* **382**, 563 (2002).
19. S. Mohanty, G. Basri, *Astrophys. J.* **583**, 451 (2003).
20. P. Padoan, A. Nordlund, *Astrophys. J.* **617**, 559 (2004).
21. A. Scholz, R. Jayawardhana, K. Wood, *Astrophys. J.* **645**, 1498 (2006).
22. J. E. Gizis *et al.*, *Astron. J.* **125**, 3302 (2003).
23. H. Bouy *et al.*, *Astron. J.* **126**, 1526 (2003).
24. A. L. Kraus, R. J. White, L. A. Hillenbrand, *Astrophys. J.* **633**, 452 (2005).
25. E. L. Martin, D. Barrado y Navascués, I. Baraffe, H. Bouy, S. Dahm, *Astrophys. J.* **594**, 525 (2003).
26. K. L. Luhman, *Astrophys. J.* **614**, 398 (2004).
27. H. Bouy *et al.*, *Astron. Astrophys.* **451**, 177 (2006).
28. G. Chauvin *et al.*, *Astron. Astrophys.* **425**, L29 (2004).
29. G. Lodato, E. Delgado-Donate, C. J. Clarke, *Mon. Not. R. Astron. Soc.* **364**, L91 (2005).
30. K. N. Allers, Ph.D. thesis, University of Texas, Austin (2005).
31. This paper is based on observations collected at the European Southern Observatory, Chile, under programs 276.C-5050 and 277.C-5012. We thank the ESO staff for carrying out the observations in service mode and making the data available to us quickly. This research was supported by a Natural Sciences and Engineering Research Council of Canada grant and University of Toronto startup funds to R.J.

#### Supporting Online Material

[www.sciencemag.org/cgi/content/full/1132128/DC1](http://www.sciencemag.org/cgi/content/full/1132128/DC1)

Materials and Methods

Table S1

References

5 July 2006; accepted 24 July 2006

Published online 3 August 2006;

10.1126/science.1132128

Include this information when citing this paper.

## 50-Ma Initiation of Hawaiian-Emperor Bend Records Major Change in Pacific Plate Motion

Warren D. Sharp<sup>1\*</sup> and David A. Clague<sup>2</sup>

The Hawaiian-Emperor bend has played a prominent yet controversial role in deciphering past Pacific plate motions and the tempo of plate motion change. New ages for volcanoes of the central and southern Emperor chain define large changes in volcanic migration rate with little associated change in the chain's trend, which suggests that the bend did not form by slowing of the Hawaiian hot spot. Initiation of the bend near Kimmei seamount about 50 million years ago (MA) was coincident with realignment of Pacific spreading centers and early magmatism in western Pacific arcs, consistent with formation of the bend by changed Pacific plate motion.

The Hawaiian-Emperor chain consists of at least 129 volcanoes and stretches for more than 6000 km across the northern Pacific basin. The Hawaiian chain is the archetypal example of a hot spot track formed as the Pacific plate moved over a mantle mag-

ma source (1). One of the most distinctive features of the chain is the Hawaiian-Emperor bend (HEB) (Fig. 1), which has been widely interpreted to indicate a major change in the direction of Pacific plate motion based on a fixed-hot spot frame of reference (2). Features

expected to accompany such a shift in Pacific plate motion are lacking at 43 million years ago (Ma) (3), the previously accepted age of the HEB (4). Paleomagnetic observations show that the Hawaiian hot spot moved rapidly southward during formation of the Emperor chain and may have become nearly fixed thereafter (5, 6). It has therefore been suggested that the HEB primarily reflects cessation of rapid hot spot motion rather than changed Pacific plate motion (3, 5). Nonetheless, both hot spot motion and changed Pacific plate motion at the HEB are indicated by analysis of global plate circuits (7). We present new ages for Hawaiian-Emperor seamounts, suggest a revised position for bend initiation, and develop their implications for the origin of the HEB.

An extensive body of radioisotopic ages was developed for the islands and seamounts of the Hawaiian-Emperor chain during systematic dating campaigns in the 1960s to 1980s (4, 8). These ages confirmed an important prediction of the hot spot hypothesis, showing that the volcanoes of the chain become progressively older with distance from the currently active hot spot under Hawaii. However, the early ages include many conventional K-Ar and  $^{40}\text{Ar}/^{39}\text{Ar}$  total fusion analyses on whole rocks that lack internal reliability criteria, making their accuracy difficult to assess. Continuing improvements in  $^{40}\text{Ar}/^{39}\text{Ar}$  extraction line-mass spectrometer systems and analytical protocols have reduced sample size requirements and increased reliability and precision. We have dated individual dredged pebbles and small pieces of drill core by the  $^{40}\text{Ar}/^{39}\text{Ar}$  method via broad-beam laser incremental heating applied to plagioclase, anorthoclase, and amphibole. Even in cases where whole rocks are moderately to highly altered, the feldspars and amphiboles separated from them typically have little or no alteration (4); thus, the new dates provide reliable ages where, in some cases, none have previously been available (9).

The sample collection that we have drawn upon has been accumulated over many years and includes dredged samples from seven cruises (9) and core from Ocean Drilling Program Leg 55. To date former locations of the hot spot as closely as possible, we have analyzed samples that can be assigned on the basis of their chemical compositions, mineralogy, and mineral chemistry to distinctive stages in the development of Hawaiian-Emperor volcanoes (4). We report new  $^{40}\text{Ar}/^{39}\text{Ar}$  ages for eight eruptive centers that have been mea-

sured on shield or postshield lavas with a single exception (Table 1). On the basis of geologic studies and modeling of volcanoes in the Hawaiian Islands, such lavas erupt while a volcano traverses the hot spot in  $\sim 1$  million years (My) (10). The duration of shield and postshield magmatism may be greater than in the Hawaiian Islands at volcanoes formed in segments of the seamount chain characterized by slower plate-hot spot motion (e.g., the HEB) or more widely spaced volcanoes (e.g., the central Emperor chain). We therefore

conservatively estimate that shield and postshield lavas were erupted at each volcano for up to 2 My. We assume that dredging or deep-sea drilling has accessed lavas only from the younger half of this interval. Accordingly, we assign a geological uncertainty of 1 My to shield and postshield lavas to reflect that they formed somewhat after passage over the hot spot's center. This geological uncertainty is asymmetric (occurring only on the older side of the measured age), is larger than the  $^{40}\text{Ar}/^{39}\text{Ar}$  measurement errors, and was com-

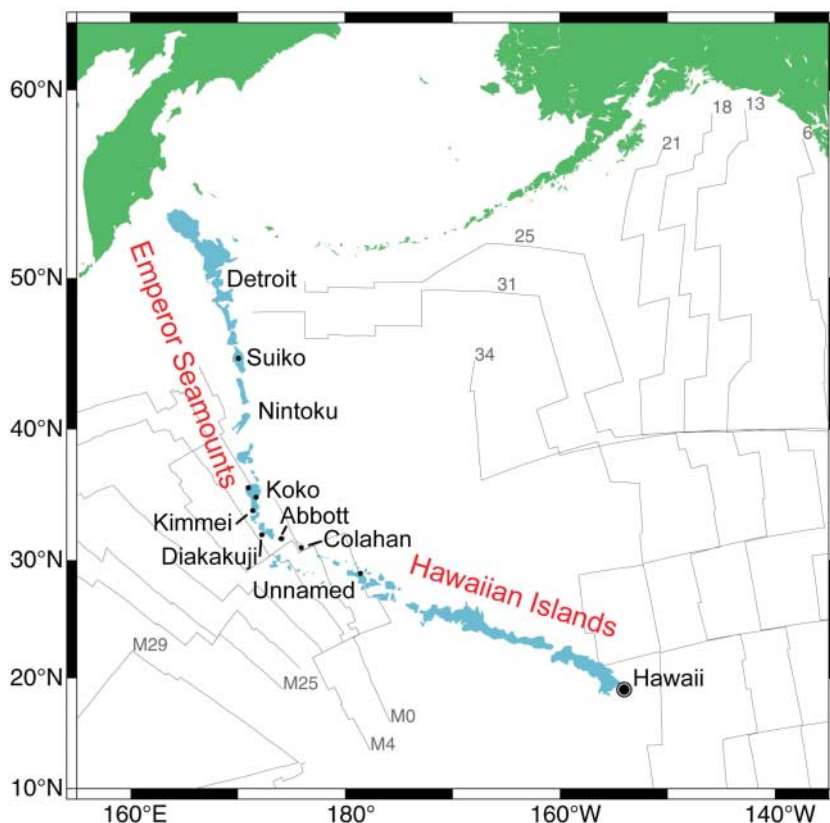


**Fig. 1.** Map of the northwestern Pacific basin. Seamounts and islands of Hawaiian-Emperor chain are shown in blue. Small circles show locations of samples dated in this study. Gray lines show sea floor magnetic anomalies labeled with chrons of the geomagnetic polarity time scale.

**Table 1.** Summary of weighted mean  $^{40}\text{Ar}/^{39}\text{Ar}$  ages for Hawaiian-Emperor seamounts.  $n$  = number of reliable ages obtained for each eruptive center; stage refers to stage of volcanism dated by analogy with volcanoes of the Hawaiian Islands (4); distance is measured along the chain from Kilauea (4). Ages were calculated using an age of 28.02 Ma for the Fish Canyon sanidine standard; decay constants, isotopic abundances, and criteria for reliable ages are given in (9).

Seamount	Age $\pm 2\sigma$ (Ma)	$n$	Stage	Distance from Kilauea (km)
Suiko	$60.9 \pm 0.3$	3	Shield and postshield	4860
Koko (north)	$52.6 \pm 0.8$	1	Shield	3812
Koko (south)	$50.4 \pm 0.1$	5	Postshield	3758
Kimmei	$47.9 \pm 0.2$	1	Postshield	3668
Diakakuji	$46.7 \pm 0.1$	3	Shield	3493
Abbott	$41.5 \pm 0.3$	1	Shield	3280
Colahan	$38.7 \pm 0.2$	4	Rejuvenated	3128
Unnamed	$31.0 \pm 0.2$	1	Postshield	2600

<sup>1</sup>Berkeley Geochronology Center, 2455 Ridge Road, Berkeley, CA 94709, USA. <sup>2</sup>Monterey Bay Aquarium Research Institute, 7700 Sandholdt Road, Moss Landing, CA 95039, USA.

\*To whom correspondence should be addressed. E-mail: wsharp@bgc.org

binned quadratically with measurement errors to give total uncertainties (table S1). The single rejuvenated-stage lava we have dated is readily distinguished from shield and postshield lavas (4) and has been assigned a geological uncertainty of 5 My.

Our new ages for Hawaiian-Emperor volcanoes plotted as a function of distance from the active Hawaiian hot spot at Kilauea further confirm a monotonic increase in age along the chain, although rates of migration of the volcanism vary considerably (Fig. 2). Such a monotonic age progression distinguishes the Hawaiian-Emperor chain from some other Pacific seamount chains such as the Line Islands and Gilbert Ridge, which have more complex age patterns and may have formed in response to local lithospheric extension (11, 12). Mean volcanic migration rates increased along the Emperor seamounts from Detroit to Koko, slowed markedly north of the HEB, and remained slow and relatively uniform through the HEB and beyond. Rates in the southern Emperors greatly exceed the hot spot's mean southward motion from Detroit to Koko determined from paleomagnetic inclination changes ( $4.3 \pm 2.3$  to  $5.8 \pm 1.9$  cm/year) (6, 13). Accelerating motion of the Pacific plate, the hot spot, or both are required in the central Emperor chain, followed by slowing of the same at or before Koko. That these highly variable motions are not associated with deviations in the trend of the Emperor chain indicates that Pacific plate and hot spot motions must have been directed essentially along the trend of the chain. If so, the HEB cannot have been produced, as previously suggested (3, 5), by slowing of the hot spot. Furthermore, if the HEB reflects primarily slower southward motion of the hot spot, the rate of volcanic migration should have slowed through the HEB as hot spot motion diminished. Contrary to this prediction, volcanic migration through the HEB is approximately constant within the limits of our data (Fig. 2). The alternative hypothesis—that the HEB formed primarily by Pacific plate motion change—is examined below in light of our new ages.

The age of the HEB is critical to assessing its relation to other events on and around the Pacific plate. An age of 43 Ma for the HEB (4, 14) has long been accepted; however, our new  $^{40}\text{Ar}/^{39}\text{Ar}$  dates indicate older ages for HEB volcanoes. Moreover, the new ages reveal that the HEB formed over a period of several million years; thus, the HEB's age is critically dependent on which part of it is considered. The 43 Ma date for the HEB was determined for its geometric apex near Diakakuji seamount. Initiation of the HEB occurred north of Diakakuji, near Kimmei seamount, where the chain's trend rotates from nearly due south to southeasterly (4). Postshield alkalic basalt from Kimmei seamount yields an age of  $47.9 \pm$

0.2 Ma, providing a minimum age for HEB initiation. An age of  $50.0 \pm 0.9$  Ma, our preferred estimate for HEB initiation, is obtained by interpolating Kimmei's shield formation age from dated shield-stage lavas at adjacent seamounts (e.g., Koko's northern eruptive center, Diakakuji, and Abbott seamounts) (Fig. 2).

HEB initiation at 50 Ma coincided with a major reorganization of northern Pacific spreading centers between seafloor magnetic anomalies 22 and 24 (15), corresponding to 49 to 53 Ma on the geomagnetic polarity time scale (16). Initiation of magmatism in the Izu-Bonin-Mariana (IBM) arc systems that extend for 2200 km along the western edge of the Pacific plate was likely marked by eruption of compositionally and mineralogically distinctive volcanic rocks with ages as old as 50 Ma (9, 17, 18). Geologic relations (19, 20) and dynamic models (21, 22) of IBM subduction initiation show that the IBM arcs likely originated by nucleation of subduction along northerly trending fracture or transform zones. This relation implies that a major shift in Pacific plate motion was associated with IBM initiation. If so, Pacific plate motion would have become more westerly upon development of self-sustaining subduction along the IBM arc system, consistent with the Hawaiian-Emperor track after the HEB (23). Reorganization of Pacific spreading centers and reconfiguration of western Pacific plate margins are expected features of a major shift in Pacific plate mo-

tion (3, 15) but have previously been considered older than the HEB. Coincident inception of the HEB at 50 Ma therefore supports a causal link among onset of subduction beneath the IBM arc, reorganized spreading, Pacific plate motion change, and formation of the HEB.

Formation of the HEB by a change in Pacific plate motion has previously been considered too rapid to be caused by buoyancy forces generated from mantle convection (24, 25), manifested primarily as slab pull (23). Until now, however, the time scale of HEB formation has not been well resolved. The new dates for HEB volcanoes show that formation of the HEB lasted for  $>8$  My—that is, from HEB initiation ( $50.0 \pm 0.9$  Ma) to eruption of shield lavas at Abbott seamount near the HEB's terminus ( $41.5 \pm 0.3$  Ma). HEB formation, and by inference associated Pacific plate motion change, was therefore considerably slower than previously appreciated, making it compatible with evolution of plate buoyancy forces, particularly pull from negative slab buoyancy expected to develop in the first few million years after initiation of IBM subduction (22). Early Eocene initiation of the  $>2600$ -km Tonga-Kermadec arc in the southwestern Pacific may also have contributed to redirection of Pacific plate motion (26). In sum, the geometry, age, and tempo of formation of the HEB are broadly consistent with those expected from changes in Pacific plate motion induced by the onset of self-sustaining sub-

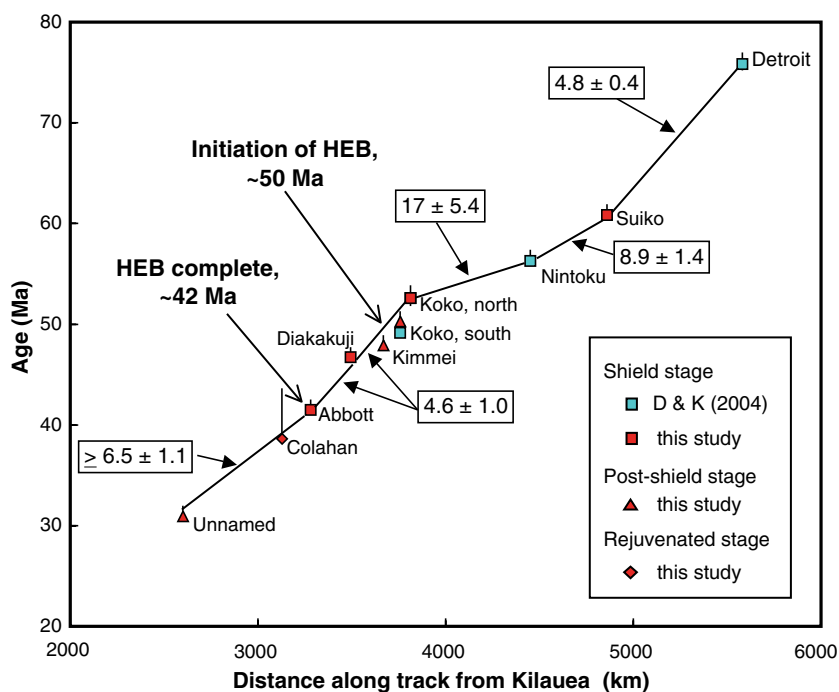


**Fig. 2.**  $^{40}\text{Ar}/^{39}\text{Ar}$  ages of Hawaiian-Emperor volcanoes plotted against distance along the chain from the modern hot spot at Kilauea volcano. Age errors shown include geological uncertainties, as discussed in the text and (9). Boxed values are volcanic migration rates for respective segments of the Hawaiian-Emperor chain in cm/year. Previously published ages (blue symbols) are from Duncan and Keller (29).

duction in early Eocene nascent arcs of the western Pacific.

A key remaining question concerns the cause of forced convergence that modeling indicates was needed to kick-start IBM subduction (21). The straight track of the Hawaiian-Emperor chain from Suiko ( $60.9 \pm 0.3$  Ma) to Koko's southern summit ( $50.4 \pm 0.1$  Ma) does not record changes in the direction of Pacific plate motion; therefore, motion change in the Eurasian or Australian plates adjoining to the west may be indicated. Possible triggers for such change are the lockup of the India-Eurasia collision zone (4, 27), which is approximately dated by the onset of major crustal shortening in that region at  $\sim 50$  Ma (28), and rifting of Australia from Antarctica, leading to convergence between the Australian and Pacific plates (23).

#### References and Notes

1. J. T. Wilson, *Can. J. Phys.* **41**, 863 (1963).
2. W. J. Morgan, *Nature* **230**, 42 (1971).
3. I. O. Norton, *Tectonics* **14**, 1080 (1995).
4. D. A. Clague, G. B. Dalrymple, *U.S. Geol. Surv. Prof. Pap.* **1350**, 5 (1987).
5. J. A. Tarduno, R. D. Cottrell, *Earth Planet. Sci. Lett.* **153**, 171 (1997).
6. J. A. Tarduno *et al.*, *Science* **301**, 1064 (2003); published online 24 July 2003 (10.1126/science.1086442).
7. B. Steinberger, R. Sutherland, R. J. O'Connell, *Nature* **430**, 167 (2004).
8. I. McDougall, *Bull. Geol. Soc. Am.* **75**, 107 (1964).
9. See supporting material on Science Online.
10. D. J. DePaolo, E. M. Stolper, *J. Geophys. Res.* **101**, 11643 (1996).
11. A. S. Davis, L. B. Gray, D. A. Clague, J. R. Hein, *Geochem. Geophys. Geosyst.* **3**, 10.1029/2001GC000190 (2002).
12. A. A. P. Koppers, H. Staudigel, *Science* **307**, 904 (2005).
13. P. V. Doubrovine, J. A. Tarduno, *Geochem. Geophys. Geosyst.* **5**, Q11L04 (2004).
14. G. B. Dalrymple, D. A. Clague, *Earth Planet. Sci. Lett.* **31**, 313 (1976).
15. T. M. Atwater, in *The Geology of North America, The Eastern Pacific Ocean and Hawaii*, E. Winterer *et al.*, Eds. (Geological Society of America, Boulder, CO, 1989), vol. N, pp. 21–72.
16. S. C. Cande, D. V. Kent, *J. Geophys. Res.* **97**, 13917 (1995).
17. M. A. Cosca, R. J. Arculus, J. A. Pierce, J. G. Mitchell, *Island Arc* **7**, 579 (1998).
18. J. A. Pearce *et al.*, in *Proceedings of the Ocean Drilling Program, Scientific Results*, P. Fryer *et al.*, Eds. (Ocean Drilling Program, College Station, TX, 1992), vol. 125, pp. 623–659.
19. T. W. C. Hilde, S. Uyeda, L. Kroenke, *Tectonophysics* **38**, 145 (1977).
20. R. J. Stern, S. H. Bloomer, *Geol. Soc. Am. Bull.* **104**, 1621 (1992).
21. C. E. Hall, M. Gurnis, M. Sdrolias, L. L. Lavier, R. D. Muller, *Earth Planet. Sci. Lett.* **212**, 15 (2003).
22. M. Gurnis, C. Hall, L. Lavier, *Geochem. Geophys. Geosyst.* **5**, Q07001 (2004).
23. R. G. Gordon, A. Cox, C. E. Harter, *Nature* **274**, 752 (1978).
24. M. A. Richards, C. Lithgow-Bertonielli, *Earth Planet. Sci. Lett.* **137**, 19 (1996).
25. D. Bercovicci, *Earth Planet. Sci. Lett.* **205**, 107 (2003).
26. S. H. Bloomer *et al.*, in *Active Margins and Marginal Basins of the Western Pacific*, B. Taylor, J. Natland, Eds. (American Geophysical Union, Washington, DC, 1995), pp. 1–30.
27. P. Patriat, J. Ardache, *Nature* **3111**, 615 (1984).
28. A. Yin, T. M. Harrison, *Annu. Rev. Earth Planet. Sci.* **28**, 211 (2000).
29. R. A. Duncan, R. A. Keller, *Geochem. Geophys. Geosyst.* **5**, Q08L03 (2004).
30. Supported by NSF grant OCE-9911292. We thank T. Atwater, R. Duncan, M. Feinman, M. Richards, and J. Tarduno for discussions.

#### Supporting Online Material

www.sciencemag.org/cgi/content/full/313/5791/1281/DC1

Materials and Methods

Figs. S1 to S7

Tables S1 to S3

References

7 April 2006; accepted 26 June 2006

10.1126/science.1128489

## Corridors Increase Plant Species Richness at Large Scales

Ellen I. Damschen,<sup>1\*</sup> Nick M. Haddad,<sup>1</sup> John L. Orrock,<sup>2,†</sup> Joshua J. Tewksbury,<sup>3</sup> Douglas J. Levey<sup>4</sup>

Habitat fragmentation is one of the largest threats to biodiversity. Landscape corridors, which are hypothesized to reduce the negative consequences of fragmentation, have become common features of ecological management plans worldwide. Despite their popularity, there is little evidence documenting the effectiveness of corridors in preserving biodiversity at large scales. Using a large-scale replicated experiment, we showed that habitat patches connected by corridors retain more native plant species than do isolated patches, that this difference increases over time, and that corridors do not promote invasion by exotic species. Our results support the use of corridors in biodiversity conservation.

Loss of biological diversity is a leading threat to the sustainability of the biosphere (1) and is largely caused by habitat loss and fragmentation (2). Landscape corridors (strips of habitat connecting other-

wise isolated habitat patches) are hypothesized to reduce the negative effects of fragmentation by facilitating gene flow and the movement of organisms, thereby preventing local extinctions and increasing species diversity (3). Corridors have become a central feature of ecological management plans worldwide, but evidence of their effectiveness has lagged behind the push for their implementation (4).

Although a number of experimental studies have demonstrated positive corridor effects on single species (5–7), few have examined corridor effects on entire communities. All of these studies were conducted at very small spatial scales (10 cm<sup>2</sup> to 10 m<sup>2</sup>), and taken together they have yielded equivocal results (8–11).

We examined the long-term effect of corridors on plant species diversity by studying

six  $\sim 50$ -ha experimental landscapes at the Savannah River Site in South Carolina, containing both isolated and connected habitat patches (Fig. 1A). Each landscape consisted of a central patch measuring 100 m by 100 m, four surrounding patches 150 m away, and a buffer area extending  $>150$  m from these surrounding patches' furthest edges (Fig. 1A). One of the four surrounding patches was connected to the central patch by a corridor 150 m by 25 m (the "connected" patch). The other three surrounding patches were equal in area to the connected patch plus its corridor, but were unconnected. These unconnected patches were of two types: winged and rectangular. Rectangular patches were 100 m by 137.5 m; the additional 37.5 m relative to the 100-m-by-100-m central patch controlled for the increased area provided by the connected patch's corridor. Winged patches were 100 m by 100 m, with two 25-m-by-75-m projections off of opposite patch sides to control for the area of the connected patch's corridor and to allow examination of the elongation in patch shape associated with corridors. Winged and connected patches had equal edge-to-area ratios. Patch and corridor dimensions were chosen because they are within the range of typical U.S. Forest Service (USFS) management activities. Further explanation of the experimental design is provided elsewhere and in the supporting online material (6, 12).

All plant species were surveyed in each patch from 2000 to 2005, except in 2004, when patches were burned by the USFS as part of restoration management (12). Our patches were open habitats with young longleaf pines

<sup>1</sup>Department of Zoology, North Carolina State University, Raleigh, NC 27695–7617, USA. <sup>2</sup>Department of Ecology, Evolution, and Organismal Biology, Iowa State University, Ames, IA 50010, USA. <sup>3</sup>Department of Biology, Box 351800, University of Washington, Seattle, WA 98195–1800, USA. <sup>4</sup>Department of Zoology, Post Office Box 118525, University of Florida, Gainesville, FL 32611–8525, USA.

\*To whom correspondence should be addressed. E-mail: damschen@nceas.ucsb.edu

†Present address: National Center for Ecological Analysis and Synthesis, 735 State Street, Suite 300, Santa Barbara, CA 93101, USA.

‡Present address: Department of Biology, Box 1137, Washington University, St. Louis, MO 63130, USA.